FUDMA Journal of Sciences (FJS)
ISSN online: 2616-1370
ISSN print: 2645 - 2944
Vol. 10 No. 15, August, 2026, pp 151 – 164
DOI: https://doi.org/10.33003/fjs-2026-1015-5883

Optimal Biomass Oil Output of Ozoro Jatropha Seed and its Thermal Analysis for Industrial Utilization

Sunday Chukwuka Iweka

Department of Mechanical Engineering, Southern Delta University, Ozoro, Delta State.

*Corresponding authors' email: iwekasc@sdu.edu.ng, chukaiweka@yahoo.com

Received: 20 July 2026
Accepted: 27 Aug. 2026
Published: 03 Sept. 2026

ABSTRACT
Biomass oil from non-edible materials is an eco-friendly approach to generating low-cost bio-lubricants and their conversion into biodiesel to power machines. First, the Jatropha Seed was dried at 169 °C, as reported by TGA (Thermogravimetric Analysis), in an oven and ground into a fine powder. The Biomass oil was extracted from the ground Jatropha Seed using BBD (Box-Behnken Design) parameters and Soxhlet equipment. The best experimental result was obtained at 60 minutes, 50 g, and 230 mL n-hexane, yielding a response of 62.66 wt.% as the highest centre-point and 47.30 wt.% as the mean optimum point. This BBD yield was validated with RStudio predictive tools. Additionally, this work revealed that OJS weight and n-hexane, their coefficient and quadratic terms, were influential, unlike time. Thus, the R2 of RStudio and the Box-Behnken Design are in alignment at 98.37%. The RStudio visualization plots aligned with the derived BBD visualization plots, making the BBD an ideal experimental tool for optimizing and predicting crude biomass oil yield, while the RStudio tool is ideal for predicting crude biomass oil yield. The seed`s higher heating and lower heating values of 30.167 MJ/kg and 29.936 MJ/kg, respectively, revealed that the seed could serve as solid biomass fuel. Furthermore, the fuel grades of the crude biomass oil derived suggest that it has good potential as a biodiesel feedstock.

Keywords: Optimization, Thermal Analysis, Ozoro Jatropha Seed Biomass Oil, Characterization, Higher Heating Values

INTRODUCTION

Utilization of fossil (hydrocarbon) products to drive energy utilities has been helpful to humankind, but their emissions have been a cause for concern, coupled with their reservoir depletion (Ruatpuia et al., 2024; Oehlschlaeger et al., 2013). In addition, with an increase in energy utility globally (Maftuchah et al., 2020) and a production decline of 28% from the year 2015 to the year 2040 (Ruatpuia et al., 2024), triggering a high cost of purchasing fossil fuel products like oil, petrol, kerosene, etc., and forces hardship on the populace (Iweka et al., 2026). There is a need for an alternative source to cushion hardship and global warming from environmental degradation caused by emissions from fossil (hydrocarbon) products (Iweka et al., 2023; Riayatsyah et al., 2022; Alhassan et al., 2024). Crude biomass oil as an alternative source can be derived from inedible seeds, microalgae, and edible seeds, but inedible seeds have been judged ideal because they pose no food challenge, are harvested at low or no cost, and are readily available (Riayatsyah et al., 2022; Yusuff, 2021). Although other clean energy sources for energy utilities are derived from wind, geothermal, hydro, solar, and biomass energy (biogas, biomass oil, biodiesel, bioethanol, biochar), but crude biomass oil remains unique because of the ease of production and its utilization, especially for transport (Ruatpuia et al., 2024; Iweka et al., 2025a; Iweka et al., 2025b).

Utilization of crude biomass oil from inedible seeds is not new because some researchers have documented findings from Jatropha seed with hexane (Ruatpuia et al., 2024; Kethobile et al., 2020), Jatropha via pyrolysis, a thermochemical process (Fortunate & Kishore, 2021), yellow oleander seed with acetone (Iweka et al., 2025a), rubber-yellow oleander seed (Abiodun & Betiku, 2022). Iweka et al. (2025a), Iweka et al. (2024), Kethobile et al. (2020), and Maftuchah et al. (2020) documented that no land portion has the same soil composition, and the soil composition of a region can impact the quality of the seed due to the effect of environmental elements like pH, Soil texture, Organic content, microbes, and contaminants. Additionally, other factors that can alter the quality of crude biomass oil include the extraction technique, the solvent used, the extraction temperature, the particle (ground) size, the seed type, the processing time, etc. (Iweka et al., 2023; Iweka et al., 2025a).

Jatropha, referred to as Jatropha *curcas*, from the Euphorbiaceae family, is a flower-bearing plant with seeds (Keneni et al., 2021). The seed is unique because the shrub can be cultivated in different types of land, including dry land, as an evergreen shrub (Kethobile et al., 2020; Keneni et al., 2021). It is usually found in countries like Ethiopia, Mexico, India, Nigeria, Brazil, Malaysia, Botswana, Thailand, Indonesia, etc. (Ruatpuia et al., 2024; Kethobile et al., 2020; Suttibak et al., 2024). Jatropha, a perennial shrub/tree (Kethobile et al., 2020), is mainly used for land demarcation in most semi-urban and rural places in Nigeria (Alpandi et al., 2022). The tree has seeds. The production of biomass oil leaves behind valuable materials for energy utilities such as the outer coat (shell), inner shell, and the seed cake (Hassan, 2022). It has been reported that biomass oil from Jatropha seed has been used as feedstock for biodiesel, medicines, and cosmetics (Kethobile et al., 2020; Odetoye et al., 2018), and its shell/coat as manure in farms (Silva et al., 2020). Jatropha seed, an inedible seed, is rich in oil due to the presence of esters but contains toxic elements (Kethobile et al., 2020; Ceran et al., 2025). Additionally, it has been documented that the by-product (seed cake) from the biomass oil recovery approach can be employed as solid biomass fuel or as biogas for cooking, transport, and heating, which makes it a viable source of energy (Kethobile et al., 2020; Odetoye et al., 2018).

The biomass oil from Egypt, as documented by Khater et al. (2024), has an oil content of 30–50%. Justifying the effect of the extraction device, soil composition, solvent used, temperature, and particle (ground) size.

There are various methods of extracting biomass oil from oilseeds, such as pyrolysis, microwave, mechanical screw, supercritical, and Soxhlet techniques, etc. (Yusuff, 2021; Kethobile et al., 2020). Still, the Soxhlet approach is preferable despite its demerits like long operating time, high operating temperature, solvent separation, and refining processes, because, apart from higher biomass oil extraction output, it's always accessible and available (Iweka et al,. 2025a). Keneni et al. (2021) worked on Jatropha seeds from two locations in Ethiopia using different solvents such as n-heptane, diethyl ether, n-hexane, and ethanol; since the soil composition is not the same, the quality would not be the same. He documented that n-hexane performed better, corroborated by Yusuff (2021). Also, Silva et al. (2020) documented the proximate and ultimate analysis of the Brazil seed.

From the literature, it has been noted that various optimization approaches have been deployed in the extraction of inedible seed biomass oil. Iweka et al. (2023) utilized Box-Behnken Design (BBD), a subset of Response Surface Methodology (RSM), with Machine Learning (Jupyter Notebook) via Python Coding in the optimization of Pawpaw biomass oil, but Jupyter Notebook performed better. Yusuff (2021) optimized Jatropha biomass oil extracted with hexane via central composite design, with an output of 56.7% biomass oil. Nyorere et al. (2024)

compared the optimal effect of extracting Pawpaw biomass oil with BBD and Artificial Neural Network (ANN), but ANN performed better. Also, Iweka et al. (2024) compared ANN with Jupyter Notebook via Python Coding, but Jupyter performed better. Although RSM comprises other packages other than BBD, BBD is considered because it`s economical in its runs. Since this investigation is centred on crude biomass oil output, BBD will be utilized. Additionally, RStudio is another machine learning prediction tool, and no researcher has validated the optimal performance of crude biomass oil from BBD with RStudio, nor carried out the seed characterization using Thermogravimetric Analysis (TGA) and Fourier Transform Infrared Spectroscopy (FTIR). The TGA detects the best temperature to dry the moist seed before crushing. The FTIR detects the functional category and existence of esters, if any, while the HHV (higher heating value) and LHV (lower heating value) will be computed from the Proximate and Ultimate analysis of the Ozoro Jatropha seed via Suttibak et al. (2024) mathematical approach. Note: Ozoro Jatropha *curcas* means it was harvested from the Ozoro region. Thus, the need to: (i) compare the new extraction parameters deployed and the physicochemical details of the crude biomass oil of the crushed seeds with other findings. (ii) Document the Thermogravimetric analysis (TGA), the Fourier Transform Infrared Spectroscopy (FTIR), and compare the HHV and LHV of the crushed seed with previous studies. (iii) Validate the predicted BBD results of the crude biomass oil with RStudio-predicted results. These outcomes will justify whether the Ozoro Jatropha seed has good potential as a solid fuel, crude biomass oil, and biodiesel feedstock, since geographical location, soil composition, solvent type, extraction equipment, temperature, seed weight and particle size, time, etc., influence optimal crude biomass oil yield and quality.

MATERIALS AND METHODS

Gathering of Materials

Jatropha seeds were collected from Esime Street, Ozoro. All compounds employed for the proximate and ultimate analyses of the crushed Ozoro Jatropha seed (OJS), physicochemical characterization, and biomass oil recovery (extraction) were of diagnostic (analytical) grade.

Instrumentation

The instrumentation employed in this work includes: Soxhlet equipment [500 mL], a 10000 W blender and crusher, an electrothermal heater of 250 mL, sieving paper, bottom flasks, funnel, measuring cylinder, automatic timer, digital weighing balance, and sample storage bottles. Others include Agilent Technologies for Fourier Transform Infrared (FTIR), the Standard gravimetric method of ASTM D-3172 for proximate analysis, LECO CHNS 2000 (ASTM D-3174-76) Elemental Analyzer (Ultimate analysis), oven, and 2950 TGA V5.4A for TGA analysis.

Method

The obtained Jatropha Seeds (OJS) was collected from Ozoro, and it was stored under a roof to avoid additional moisture. The shells were removed, and the fresh OJS, as displayed in Fig. 1, was processed further by drying in an oven; after drying, it was ground to a smooth form using a KENWOOD grinder, but it stuck together due to its oiliness, as described in Figure 2.

Figure 1: Fresh Ozoro Jatropha Seed

Figure 2: Ground OJS

Thermogravimetric Analyzer (TGA) of the Ground OJS
2950 TGA V5.4A was deployed to generate an ideal temperature for removing water from OJS with the help of a thermal chamber (oven) to obtain the OJS weight at equilibrium. The TGA was operated at approximately 169 ºC to check its decomposition behaviour from 22 ºC to 1000 ºC and document the results.

FTIR of the Ground OJS
Agilent Software was used to analyze the functional groups observed in the ground OJS. The 0.01 g of pulverized OJS that was collected was homogenized with 0.01 g of anhydrous KBr using an agate mortar. The combinations were compressed with a vacuum hydraulic press (Graseby Specac) at 1.2 psi to produce a transparent pellet. An electronic analyzer that detailed the spectrogram of the tested ground OJS disclosed the scanned sample's path through the infrared. The ground OJS was scanned in the absorbance range of 4000 cm^{-1} to 650 cm^{-1}. The specific functional groups, chemical form, and molecular binding configuration of the ground OJS under examination served as the basis for the spectrum type.

Proximate Procedure
The proximate analysis is made up of the moisture content, ash, volatile matter, and fixed carbon.

Moisture Content (MC)
The samples' moisture content was computed to assess the weight loss after 10 minutes at 169 ℃ under N_2 purge. About 0.5 g of the air-dried biomaterials was placed inside a pottery crucible. The biomaterials were placed inside a Lindberg muffle furnace that had been purged with N_2 gas for at least 20 minutes at a flow rate of 3 L/min for the swift removal of all oxygen. After 10 minutes of heating at 169 ℃, the furnace was turned off, and the biomaterials (samples) were immediately transferred to a desiccator to cool for an hour before being evaluated in accordance with Eq. 1.

$$MC = \frac{M - Q}{M} \times 100 \quad (1)$$

where M is the air-dried OJS weight
Q is the dried OJS weight at 169 ℃ via an Oven
MC = Moisture content.

Volatile Matter (VM)
The dried biomaterial (sample) was heated to 850℃ under N_2 purge to ascertain the volatile matter present. While they were heating, the crucibles holding the biomaterials were kept in a stainless steel dish inside a muffle furnace and covered with a pottery (ceramic) cover. Through a tiny opening in the dish cover, a thermocouple and N_2 purge line were passed through the top of the furnace and down into the stainless steel dish. For approximately five minutes, the dish was purged using N_2 gas at a flow rate of 5 L/min. After the first purge, the furnace was turned on after the N_2 flow rate was reduced to 3 L/min, and the furnace was adjusted to the necessary peak separation temperature. Additionally, the temperature within the stainless steel dish was tabulated every 60 seconds during the heating stages. The furnace lock was opened, and the furnace was turned off when the temperature inside the stainless steel dish reached the separation temperature of 850 ◦C. Once the crucibles were weighed in accordance with Eq. 2, the N_2 purge in the stainless steel dish was retained (3 L/min) throughout cool-down hours (2–4 h).

$$\text{Volatile matter} = \frac{M - B}{M} \times 100 \quad (2)$$

Where M is the air-dried OJS weight of the biomaterial
B is the OJS weight at 850 ℃ via a furnace.

Ash Value (AV)
The biomaterial`s ash value was derived by heating the biomaterial to 995 ℃ using the furnace as recommended by the TGA. The crucible covers were removed to ensure complete combustion, and a low flow of house air (1.5 L/min) was used to continuously clean the furnace. The furnace attained 995 ℃, and this temperature was maintained for 10 minutes. Once the ash formed, the samples were transferred to a desiccator and allowed to cool for an hour after the furnace was shut off. The amount of ash was computed by subtracting the weight of the empty crucible from the weight of the crucibles containing the ash. Furthermore, evaluations were performed in triplicate for all proximate analyses as indicated in Eq. 3.

$$AV = [\frac{D}{Q}] \times 100 \quad (3)$$

where D is the new weight of the OJS
Q is the initial weight of the OJS at 169 ℃. Ash value [%] = AV

Fixed Carbon
The fixed carbon (FC) was computed in accordance with Eq. 4. Usually, a "distinction" is employed to compute the carbon content, which means that the proportion of fixed carbon is assumed to be the leftover quantity after subtracting the sum of VM and AV from 100.

$$F = 100 - (VM + AV) \quad (4)$$

Ultimate Analysis
This was processed to obtain nitrogen, hydrogen, sulphur, and carbon. The oxygen value available is generated by subtracting the combined values of nitrogen, hydrogen, sulphur, and carbon from 100.

Higher Heating Value (HHV) and Lower Heating Value (LHV) Procedures
The HHV and LHV using equations (5) and (6) published by Suttibak et al. [18]. Thus, this energy can be employed for heating and electricity, both for commercial and home utilities.

$$HHV\ [\frac{MJ}{kg}] = 1.3675+0.3137C+0.7009H+0.0318O \quad (5)$$

$$LHV\ [\frac{MJ}{kg}] = HHV - 2.442\times8.936\ (\frac{H}{100}) \quad (6)$$

Where S = sulphur, N = nitrogen, O = Oxygen, C = carbon content, H = hydrogen

$$O^* = 100 - S - N - C - H. \quad (7)$$

Where Eq. 7 is the oxygen content available for the OJS energy utilization.

Extraction of the Ozoro Jatropha Seed Biomass Oil
The Ozoro Jatropha Seed Biomass Oil (OJSO) was processed at the Chemical Engineering Lab, Southern Delta University, Ozoro, Nigeria. The OJSO from Esime Street, Ozoro, was extracted using analytical standard to examine its physical and chemical properties. OJSO was derived via a Soxhlet device with a calculated quantity of chemicals and reagents of analytical standard. The BBD was employed in the conceptual draft (design), while the BBD and the developed RStudio algorithm were used in the optimization of OJSO. The 15 kg OJS were thoroughly washed and rinsed in tap water. After rinsing, the thermal chamber at the recommended TGA temperature of 169 ^{O}C was utilized to dry the seeds to achieve uniform OJS weight. The volume range and concentration of n-hexane employed in this extraction period were 7500 mL and 99.5% purity, respectively.
Fig. 1 displays the freshly harvested OJS that were thermally dehydrated for this research. A 10000 W KENWOOD crusher

and blender was deployed to grind the seeds to a fine powdered form capable of being sieved by a 65-aperture mesh. The extraction elements in this study were optimized using the BBD with 17 runs. A known weight of ground OJS was placed into a quantified amount of n-hexane in the thimble of the Soxhlet device. A 500 mL flask carrying n-hexane was linked to the recovery instrument, a condenser was fixed to the other end of the recovery instrument to private spillage, and the heating mantle was powered on at 69 ^{O}C.

OJS biomass oil was extracted from the solvent following the extraction approach, and n-hexane was removed by heating the OJS biomass oil. Note that heating up to or very close to the boiling temperature (point) of an extraction solvent increases biomass oil yield, but heating above the boiling temperature (point) can cause biomass oil dryness. In this study, the n-hexane boiling point was set at 69 ^{O}C. The OJS biomass oil was then dried and quantified gravimetrically in accordance with Eq. 8.

$$Oil\ response\ (wt.\%) = \frac{y_o}{y_s} \times 100 \qquad (8)$$

Where y_o (g) depicts the OJSO weight that was recovered, and y_S (g) depicts the OJS weight that was used in recovering the OJSO.

The recovered OJSO's physical and chemical properties were determined using the ASTM approach. The properties, such as saponification value (via ASTM approach - D94 -07), peroxide content, iodine value, acid content (via ASTM approach - D974), cetane number, HHV, etc., in line with neem seed bio-oil documented by Ugye et al. (2025).

BBD and RStudio Approach

RSM from Design-Expert Version 13 is a superset of BBD and was employed in the optimization of OJSO, as indicated in Table 1. The numeric elements chosen were three (3), as the input variables are time, quantified OJS weight, and n-hexane, as showcased in Table 1, to derive a response tagged OJSO at a fixed temperature of 69 ^{o}C.

Table 1: Input Factors of BBD

	Parameter	Unit	Peak	Low
A	Time	Min	70	50
B	OJS Weight	G	60	40
C	n-Hexane	mL	260	200

RStudio is a statistical coding software, and a subset of Anaconda Navigator is the other optimization package to be used in this research. It comprises different libraries for analysis, e.g., dplyr, car, broom, readr, moments, ggplot2, psych, plotly, akima, etc. The model generated a coded quadratic equation, as displayed in Eq. 8, and Table 2 data, and plots from 17 runs. Also, the Fig. 3 schematic techniques with the BBD pattern was used to extract the OJSO.

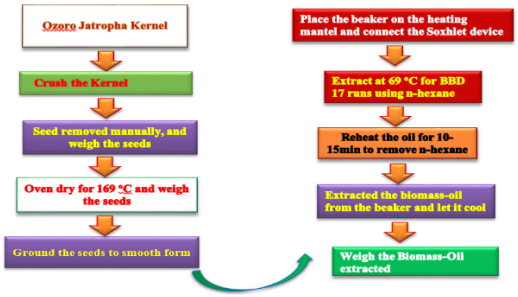

Figure 3: Schematic Techniques of the Produced OJSO

Other Factors that can affect the OJS Yield

Other factors that can alter the quantity and quality of biomass oil include extraction temperature, particle (ground) size, etc. Additionally, the extraction technique, solvent used, and seed type can alter the quality and quantity of the OJS oil (Iweka et al., 2023; Iweka et al., 2025a).

Cetane Number of the OJSO

Equation 9, as reported by Onoji et al. (2016), was used in the computation of cetane number because cetane number relies on the Iodine value (IV) and Saponification value (SV) of the OJSO produced.

$$CN = \frac{5458}{SV} + 46.3 - (IV * 0.225) \qquad (9)$$

***2.3.10** HHV (Higher Heating Value) of the OJSO*

Equation 10, as documented by Onoji et al. (2016), was used in the computation of the HHV. This revealed that the HHV relies on both the Iodine and Saponification values, just like the cetane number but with different constants.

$$HHV = -(SV * 0.041) - (IV * 0.015) + 49.43 \quad (10)$$

RESULTS AND DISCUSSION

Feedback on the Characterized OJS

The feedback of the characterized OJS is presented in the subdivisions of this section.

Ground OJS TGA Feedback

The thermogravimetric analysis machine was employed to check the optimal temperature for complete decomposition of the OJS, as showcased in Fig. 4. Thus, from Fig. 4, the dehydration commenced from 22.31 ^{o}C till the first dehydration at 168.59 ^{o}C comparably 169 ^{o}C with 11.55 % moisture dried off, with a leftover of 88.40% JOS dehydrated oil seeds to be ground, which is this study`s target. This is the point before carbon formation (Iweka et al., 2025a). The spiral in blue is the derivative OJS weight loss due to the rate of change with its corresponding temperature, while the spiral in green depicts the OJS weight loss plot (Iweka et al., 2025a). Thus, it is ideal to dry the OJS at 169 ^{o}C as detected by the TGA because this first stage, which occurred between approximately 22 °C and 169 °C, accounted for an 11.55% OJS weight loss (0.3088 mg) and corresponds to the evaporation of free and loosely bound surface moisture

together with the loss of light volatile extractives from the seed's inner light shell as displayed in Fig. 1. This stage is typically regarded as a physical dehydration step rather than real thermal decomposition because it comes before any noticeable structural degradation as displayed in Fig. 4. Hence, no meaningful thermal alteration that might impact both biomass oil yield and quality.

Additionally, the second decomposition was at 462.17 ºC with 68.22% biomass oil burnt off, leaving 20.32%. At this second phase, significant burning took place. Further away from this point is the third step decomposition, where 4.956% was burnt off as residue at 995.37 ºC, leaving 15.26% biochar waiting to completely phase off as gas as the operation continues with an increase in temperature and time. Thus, the thermal decomposition characteristics of Ozoro Jatropha seed under controlled heating comprise the first step, the second step, and the third step. From the first to the third step, there has been significant OJS weight loss due to an increase in temperature with time, as depicted in Fig. 4, leading to a reduction in volatile content with an increase in carbon deposit (Iweka et al., 2025a).

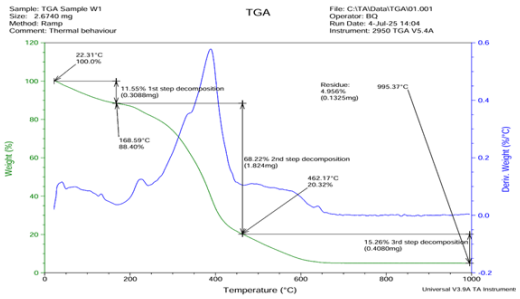

Figure 4: TGA of OJS Decompositions

OJS FTIR Feedback

The FTIR spectrum detected the functional group elements present in the OJS at wavelengths from 4000 to 650 cm^{-1}, as depicted in Fig. 5, in line with standards for organic materials (Nandiyanto et al., 2019). A broad, intense band centred at 3272.6 cm^{-1} is assigned to O–H and N–H stretching vibrations arising from hydroxyl groups in moisture, carbohydrates, and phenolics, overlapping with the N–H stretch of proteins (amide A); this broad envelope is typical of lignocellulosic, protein-bearing seed origins (Khemthong et al., 2024).

The pair of bands at 2924.1 cm^{-1} and 2853.3 cm^{-1} corresponds to asymmetric and symmetric C–H stretching vibrations of aliphatic CH_2/CH_3 groups, respectively, confirming the presence of the long-chain fatty-acid hydrocarbon backbone of the seed oil triglycerides. The weak features near 2357.5 cm^{-1} and 2149.0 cm^{-1} are commonly attributed to atmospheric CO_2 interference and are not considered structurally significant. The absorption at 1636.3 cm^{-1} is assigned to C=O stretching of the amide I band overlapping with C=C vibrational mode of unsaturated fatty acid chains, while the band at 1541.3 cm^{-1} corresponds to the amide II band of seed storage proteins; the presence of both amide I and amide II features is consistent with the appreciable protein content typical of Jatropha seed cake material (Khemthong et al., 2024).

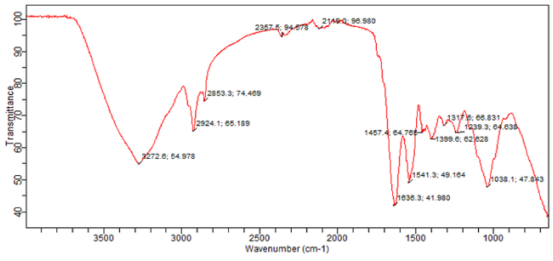

Figure 5: FTIR of OJS Compositions

The bands at 1457.4 cm^{-1} and 1399.6 cm^{-1} are associated with CH_2/CH_3 bending and O–H bending vibrations, respectively, while the peak at 1317.6 cm^{-1} and the doublet-like feature near 1239.3 cm^{-1} are attributed to C–N stretching (amide III) and C–O stretching of esters and carbohydrate ring structures. The peak at 1038.1 cm^{-1} is assigned to C–O stretching vibrations characteristic of polysaccharides (cellulose/hemicellulose) in the seed coat. Taken together, the spectrum confirms that the Jatropha seed is a composite morphology of triglyceride bio-oil, protein, and lignocellulosic carbohydrate, an interpretation that is consistent with FTIR-based characterization of Jatropha seed and seed-cake material reported elsewhere (Khemthong et al., 2024; Nandiyanto et al., 2019).

Ground OJS Proximate and Ultimate Outcome

Tables 2 and 3 display the outcomes of the needed parameters for HHV and LHV computations, respectively.

Table 2: Ground OJS Proximate Outcome

Bio-Seed (%)	Moisture	Ash	Volatile matter	Fixed carbon	HHV (MJ/kg)	Reference
This Work	4.927	2.133	18.57	74.37	30.16691	
Jatropha seed	10.3	3.00	84.5	2.3	29.3	(Silva et al., 2020)
Jatropha seed cake	1.9	15.4	53.4	29.3	21.6	(Kethobile et al., 2020)

Table 3: Ground OJS Ultimate Outcome

Biomass (%)	Carbon	Hydrogen	Nitrogen	Sulphur	Oxygen	LHVMJ/kg	Reference
This Study	88.613	1.057	0.607	0.417	8.197	29.936	
JS Brazil	46.4	5.9			43.9	28.8	(Silva et al., 2020)
JS cake Botswana	54.5	6.6	4.9		43.1	20.16	(Kethobile et al., 2020)

JS = Jatropha Seed

As indicated above, the 30.17 MJ/kg of HHV and 29.94 MJ/kg of LHV values indicate that the OJS has good potential as a solid fuel, crude biomass oil, and biodiesel feedstock. Thus, it can be processed into crude biomass oil by Soxhlet extraction, as corroborated by the FTIR result, which can serve as a bio-lubricant and as a feedstock for biodiesel.

Additionally, the HHV of 29.3 MJ/kg and LHV of 28.8 MJ/kg from Brazil Jatropha seed reported by Silva et al. (2020) and that reported by Kethobile et al. (2020) are both smaller compared to Ozoro Jatropha seed (OJS) outcomes. An indication that the biomass oil in the OJS boosted its internal energy, which is ideal for its utilization as solid biomass fuel.

Optimization Results of OJSO

The three design input elements, namely, Time of extraction, Ground OJS Weight, and n-Hexane, were optimized to determine their impact on the output of the extracted OJS biomass oil is showcased in Fig. 6. The BBD drafted seventeen (17) runs. After the recovery period, the feedback of each run is displayed as the outcome column in Table 4. Note that this biomass oil is a crude biomass oil from Jatropha seeds.

Figure 6: The Produced OJS Biomass Oil

The operation time of 60 minutes, ground OJS weight of 50 g, and n-hexane amount of 230 mL produced the peak OJS biomass oil output of 62.66 wt% in run 11. Additionally, run 2 OJS biomass oil output produced the smallest output of 27.5 wt%. at 60 minutes, 60 g of ground OJS and 200 mL of n-Hexane. Hence, this Soxhlet extraction unit approach revealed that its higher output depends on the amount of n-hexane and OJS weight as illustrated in the contour graphs in Fig. 7a, Fig. 7b, and Fig. 7c, and this aligns with Table 5. Table 4 displays the impact of the supplied (input) elements, such as time of extraction, OJS weight, and n-hexane, on their corresponding output. Table 4 is made up of OJS biomass oil Output of BBD and predicted BBD, validated with predicted RStudio output (via a Machine Statistical Software). Equation 9 displays the actual quadratic equation, and the input elements developed by BBD in Table 4 were applied in code to derive its response elements, as displayed in Table 4 and in the graphs as depicted in the next sub-headings.

Table 4: Biomass Oil Predicting and Optimization Outcome

Run	A:Time (mins)	B:Weight (g)	C:n-Hexane (ml)	OJSO Actual Output (wt.%)	Predicted BBD	Predicted RStudio
1	70	50	200	41.90	43.60	43.60125
2	60	60	200	27.50	27.89	27.88750
3	50	40	230	38.30	40.39	40.38875
4	50	50	200	42.50	41.21	41.20625
5	50	50	260	48.24	46.54	46.53875
6	60	40	260	44.00	43.61	43.61250
7	70	40	230	53.30	52.39	52.39375
8	60	60	260	38.17	38.96	38.96500
9	50	60	230	38.70	39.61	39.60625
10	60	50	230	58.55	61.21	61.21200
11	60	50	230	62.66	61.21	61.21200
12	70	50	260	46.16	47.45	47.45375
13	70	60	230	33.00	30.91	30.91125
14	60	40	200	46.30	45.51	45.50500
15	60	50	230	61.72	61.21	61.21200

Run	A:Time (mins)	B:Weight (g)	C:n-Hexane (ml)	OJSO Actual Output (wt.%)	Predicted BBD	Predicted RStudio
16	60	50	230	62.00	61.21	61.21200
17	60	50	230	61.13	61.21	61.21200

The solvent to solid ratio was considered from 3.3:1 to 6.5:1 in order to validate literatures and the maximum yield at run 11, with a ratio of 230 mL (hexane) to 50 g (OJS weight) gave 4.6:1, which is higher than 4. Thus, Table 4 confirms that for maximum yield, the ratio of solvent to weight of the ground OJS should be at least 4:1, as documented by Iweka et al. (2023). Note that the initial biomass mass was 850 g while the recovered biomass oil mass was 804.13 wt.%, as indicated in Table 4 of the total ground OJS weight and the biomass oil actual/experimental output.

Additionally, the reaction time influenced the quality and quantity of biomass oil yield because it makes the ground Jatropha seed well soaked in the extraction solvent (n-hexane).

The ANOVA was applied to detect the significant effects of the operating conditions applied in the recovery of OJSO. Table 5 displays the results of the ANOVA from the Soxhlet device approach. The Soxhlet device approach model is a vital technique in this OJSO extraction, as illustrated by its F-value of 47.05 and p-value of <0.0001. According to Iweka et al. (2023), if the p-value is below 0.05, the corresponding term is influential. OJS weight and n-hexane, their coefficient and quadratic terms, were influential, unlike time, as illustrated in Table 5.

Table 5: ANOVA Results of OJOS via Soxhlet Device

Origin	Sum of Squares	Df	Mean Square	F-value	p-value	Feedback
Model	1883.77	9	209.31	47.05	< 0.0001	Significant
A-Time	5.48	1	5.48	1.23	0.3038	Insignificant
B-OJS Weight	247.87	1	247.87	55.72	0.0001	Significant
C-n-Hexane	42.18	1	42.18	9.48	0.0178	Significant
AB	107.12	1	107.12	24.08	0.0017	Significant
AC	0.5476	1	0.5476	0.1231	0.7360	Insignificant
BC	42.06	1	42.06	9.45	0.0179	Significant
A^2	226.83	1	226.83	50.99	0.0002	Significant
B^2	716.76	1	716.76	161.13	< 0.0001	Significant
C^2	354.23	1	354.23	79.63	< 0.0001	Significant
Residual	31.14	7	4.45			
Lack of Fit	21.07	3	7.02	2.79	0.1734	not significant
Pure Error	10.07	4	2.52			
Cor Total	1914.91	16				

Additionally, an R^2 (0.9837) fell close to one and this reveals that the BBD outcome is outstanding. The difference of less than 2 between the adjusted value R^2 of 0.9626 and the predicted value R^2 of 0.8157 justifies that the model is fit. Additionally, the adequate signal of 20.601 revealed that the design can navigate the model space, which is good, as depicted in Table 6. The forecasted mean value generated 61.212 wt.% from the point forecasting (prediction) section, and this conformed with the model (design) code equation intercept of 61.21 wt.% from the polynomial equation tagged Eq. (11), in line with the standard approach for Box–Behnken-type designs applied to oil-extraction optimization (Ashine et al., 2022). The coded units revealed that the relative magnitude of each coefficient directly reflects the strength of that element's influence on the output, independent of the units of measurement.

Furthermore, the RStudio code generated from Eq. (12) comprises input and response parameters saved in an Excel CSV (Comma Delimited) sheet.

OJSO wt.% = +61.21 – a*0.8275 – b*5.57 + c*2.30 - a*b*5.17 – a*c*0.3700 + b*c*3.24 – a**2*7.34 – b**2*13.05 – c**2*9.17 (11)

a = Time of extraction, b = ground OJS Weight, c = n-hexane.

```
a = "C:\\Users\\chuka\\Desktop\\archive1\\samoil1.csv"
data <- read.csv(a)
```
(12)

Table 6: Design Fitness Variables

Elements	BBD Values	RStudio Values
Std. Dev.	2.11	2.109
Mean.	47.30	47.30
p-value	<0.0001	1.953e-05
R^2	0.9837	0.9837
R^2 Adjusted	0.9628	0.9628
R^2 Predicted	0.8157	
Adeq. Precision	20.6013	
Max.	62.66	62.66
Min.	27.50	27.50

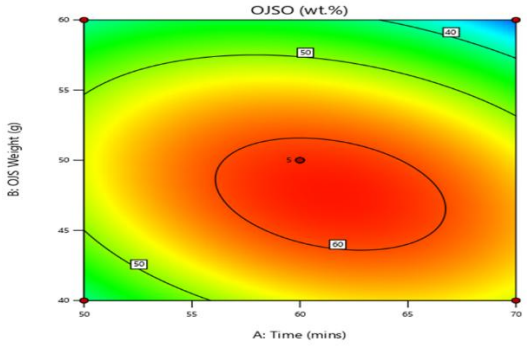

Figure 7a: BBD Graph of OJS Weight Versus Time

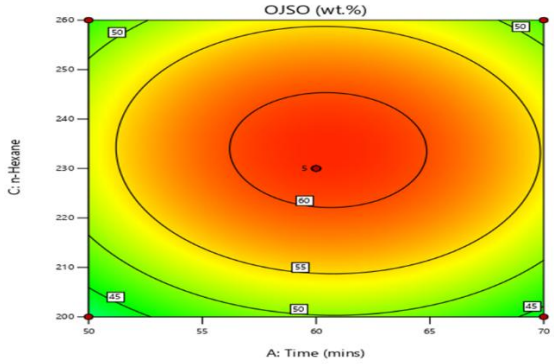

Figure 7b: BBD Graph of n-Hexane Versus Time

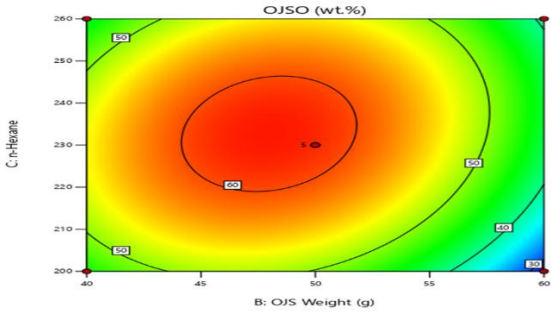

Figure 7c: BBD Graph of OJS Weight Against n-Hexane

The operating element impacts showcased in Fig. 7a, Fig. 7, and Fig. 7c agree with RStudio`s contour graph in Fig. 9a-c. Where red illustrates the point of the peak response region, yellow illustrates the region next to the peak response region, green illustrates the level of the mid response region, and blue illustrates the lowest response region.

Furthermore, the adequacy of the fitted quadratic model was further examined through standard regression diagnostic plots (Fig. 8).

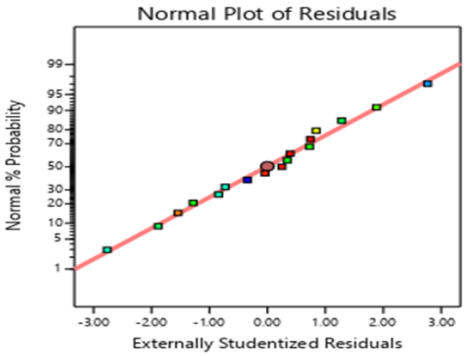

Figure 8a: Normal Probability Plot of the Externally Studentized Residuals

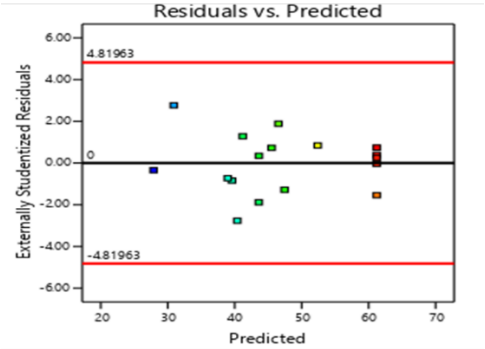

Figure 8b: Externally Studentized Residuals Versus Predicted OJSO Values

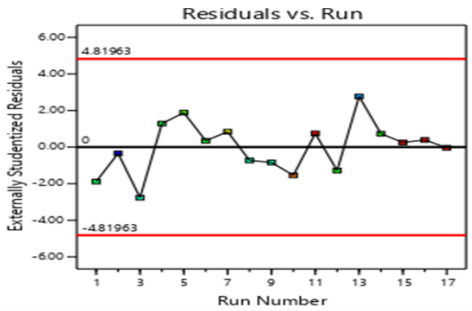

Figure 8c: Externally Studentized Residuals Versus Experimental Run Order

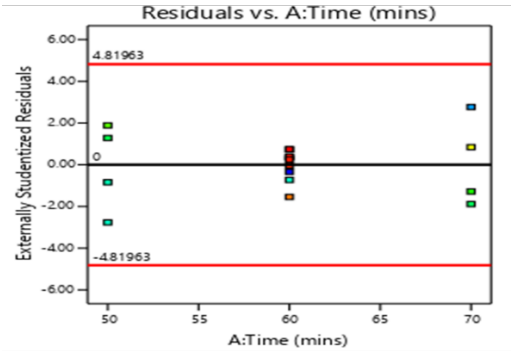

Figure 8d: Externally Studentized Residuals Versus Factor A (Time)

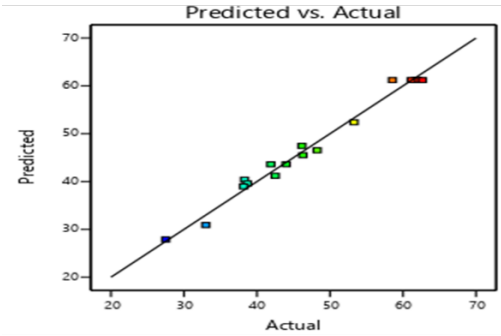

Figure 8e: Predicted Versus Actual OJSO Values

The normal probability plot (Fig. 8a) revealed that the residuals fell close to a straight line with no marked departure at either tail, supporting the assumption that the residuals are approximately normally distributed. The plot of residuals against predicted values (Fig. 8b) revealed a random scatter about zero with all points lying within the ±4.81963 outlier bounds, indicating homoscedasticity (constant residual variance) and no discernible funnel or curvature pattern that would suggest an inadequate model form. Similarly, the residuals-versus-run plot (Fig. 8c) and the residuals-versus-Factor-A plot (Fig. 8d) show no systematic trend, confirming that neither the order in which the experiments were carried out nor the extraction time introduced any hidden bias into the model. Finally, the predicted-versus-actual plot (Fig. 8e)

revealed that the experimental figures clustered closely along the 45° line of perfect agreement across the full range of the response (27.5–62.66), demonstrating good agreement between the model-predicted and experimentally observed OJSO values; these are consistent with the diagnostic criteria recommended for Box–Behnken response-surface models (Ferreira et al., 2007).

Table 7: Lack-of-Fit Analysis

Origin	Sum of Squares	Df	Mean Square	F-value	p-value	Remark
Linear	1609.31	9	178.81	71.04	0.0005	—
2FI	1459.59	6	243.26	96.64	0.0003	—
Quadratic	21.07	3	7.02	2.79	0.1734	Suggested
Cubic	0.0000	0	—	—	—	Aliased
Pure Error	10.07	4	2.52	—	—	—

The lack-of-fit analysis was deployed to check whether this Box-Behnken-type model substantially represents the figure; a not substantial lack of fit ($p > 0.05$) revealed that the model error is not significantly larger than the pure (replicate) error and that the model form is appropriate (Ferreira et al., 2007). As displayed in Table 7, the quadratic model returned a lack-of-fit p-value of 0.1734, which is not substantial relative to the pure error, while it captured markedly more of the curvature in the data than the linear model. The quadratic draft was therefore correctly selected by the software as the most appropriate model for describing the OJSO output, a conclusion in agreement with similar Box–Behnken-based bio-oil yield optimization studies in which quadratic models with non-significant lack of fit were likewise selected as the best-fitting response surface (Ashine et al., 2022).

Table 8: Developed Algorithm Elements Coefficients

Factor	Coefficient	Std. Error	CI High (95%)	CI Low (95%)	VIF
Intercept	61.21	0.9432	63.44	58.98	—
A – Time	0.8275	0.7457	2.59	−0.9357	1.0000
B – OJS Weight	−5.57	0.7457	−3.80	−7.33	1.0000
C – n-Hexane	2.30	0.7457	4.06	0.5330	1.0000
AB	−5.17	1.05	−2.68	−7.67	1.0000
AC	−0.3700	1.05	2.12	−2.86	1.0000
BC	3.24	1.05	5.74	0.7489	1.0000
A^2	−7.34	1.03	−4.91	−9.77	1.01
B^2	−13.05	1.03	−10.62	−15.48	1.01
C^2	−9.17	1.03	−6.74	−11.60	1.01

A model term is taken as statistically significant when its 95% confidence interval excludes zero, as displayed in Table 8. On this basis, the linear terms B (OJS weight) and C (n-hexane volume), the interaction terms BC and AB, and all the quadratic terms (C^2, B^2, A^2) were significant contributors to OJSO yield, whereas the linear term A (time) and the interaction term AC were not significant, since their confidence intervals span zero. The negative and comparatively large coefficient for B^2 (−13.05) revealed that OJS weight exerts the strongest curvature effect on yield among the three factors, followed by C^2 (−9.17) and A^2 (−7.34); this pattern of dominant quadratic curvature is typical of solvent-extraction processes in which yield increases with an element up to an optimum before mass-transfer or dilution limitations cause a decline (Yusuff, 2021). The negative linear coefficient for B (−5.57) together with its strongly negative quadratic term revealed that biomass oil yield falls as OJS weight increases beyond the optimal solvent-to-solid ratio, consistent with a solute-saturation effect in the n-hexane phase, while the positive coefficient for C (+2.30) confirms that increasing solvent content improves extraction efficiency by improving mass transfer of the analyte, in agreement with parametric studies of n-hexane-based Jatropha biomass oil extraction (Yusuff, 2021; Ashine et al., 2022). The negative AB interaction revealed that the beneficial effect of solvent volume is reduced at higher seed loadings, while the positive BC interaction revealed that increasing solvent volume can partly offset the yield-suppressing effect of a higher OJS weight. Variance inflation factors (VIF) of essentially 1.00–1.01 for all terms confirm the absence of multicollinearity among the model terms, indicating that the design provided orthogonal, independent estimates of each effect.

Forecasted Outcomes Validation with RStudio

RStudio is a statistical tool used to model, enhance, and predict the ideal variables that suggest the maximum outcomes. RStudio R^2 of 0.9837 in Table 6 and its actual (real) response of 62.66 wt.% in Table 4 run 11 align with the BBD R^2 and real response, respectively. These outputs are corroborated by Fig. 9a, Fig. 9b, and Fig. 9c generated by RStudio. Although BBD is the bedrock because it provides the platform (input and output data) RStudio relies on to process, the predicted output from RStudio was in line with the predicted output from BBD. Thus, its utilization promotes trending technology applications in solving issues and making validation of optimization of vital parameters reliable, especially in biomass oil industries. A great contribution to clean energy solutions and pollution mitigation.

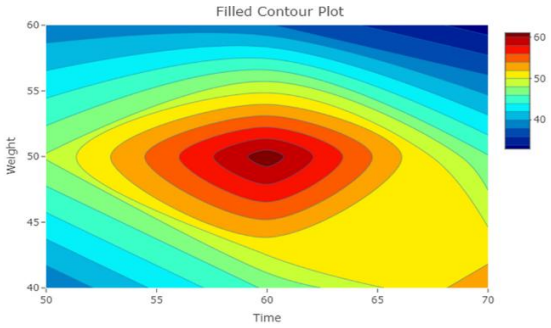

Figure 9a: RStudio Contour of OJS Weight Versus Time

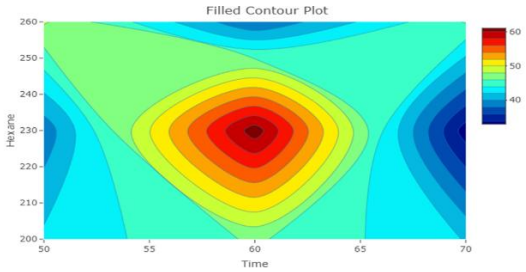

Figure 9b: RStudio of n-Hexane Versus Time

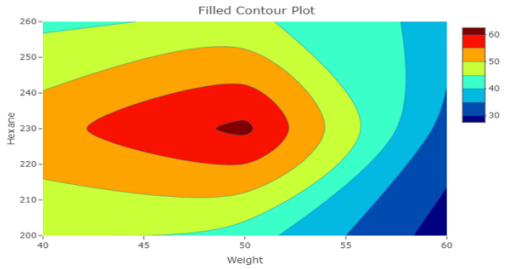

Figure 9c: RStudio OJS Weight Versus n-Hexane

Maximization of Derived Figure and its Validation

Table 4 showcases the input elements in run 11, where time is 60 mins, OJS weight is 50 g, and n-hexane is 230 mL, yielding a response of 62.66 wt.% as the highest centre-point and 47.30 wt.% as the mean optimum point both in BBD and RStudio tools. This is comparable to a repeated optimization yield of 61.14 wt.% at 60 mins, 46 g, and 229 mL. Additionally, Table 5 and Table 8 revealed that OJS weight and n-hexane are key to higher OJS oil yield. The proximate and ultimate analysis demonstrates that the OJS is rich in ester, as corroborated by the FTIR. When the ground OJS is compared with other scholars` reports on Jatropha seed and its cake, the HHV (calorific value) and LHV generate higher energy output. The TGA decomposition in Fig. 4 conforms to its moisture removal temperature of 169 ^{o}C.

Physical and Chemical Qualities of the Recovered OJSO

The physical and chemical qualities of the extracted OJSO in Table 9 explain the usefulness of the OJS as documented by (Iweka et al., 2026). The high free fatty acid value, a subset of acid value derived from OJS biomass oil, demonstrates that it is an ideal feedstock for biodiesel production, provided it`s esterified before transesterification. Additionally, since the peroxide content is <20 meq O_2kg^{-1} means it can be preserved over a long time, as corroborated by its substantial iodine content, which implies that the OJS biomass oil can be preserved at room temperature as a liquid without turning into wax, as described in Table 9. The moisture value of 0.002% implies it can be used as a lubricant without corroding the engine or electronic parts. The physical and chemical qualities of OJS biomass oil align with other scholars` findings in Table 9. Moreover, specific gravity between 0.82 to 1.07 from crop biomass oils is tagged as a good green fuel source (Iweka et al., 2026). Additionally, Haq et al. (2023) from Pakistan obtained 32.5 wt.%, Yusuff (2021) from Ado-Ekiti, Nigeria used n-hexane and generated 58.98wt.%, Maftuchah et al. (2020) from East Java, Indonesia produced 47.58wt.% biomass oil via a mechanical technique. Also, Emil et al. (2010) investigated Thailand and Malaysia seeds using n-hexane, and the biomass oil output was 64.23 wt.% and 63.16 wt.%, respectively. But the OJS biomass oil using n-hexane yielded 62.66 wt.%, which is greater than the Jatropha biomass oil from Ekiti, Nigeria, and Java, Indonesia, but very close to those produced from Thailand and Malaysia seeds. Thus, Table 9, as documented by Maftuchah et al. (2020) and Emil et al. (2010), confirms Kethobile et al. (2020) and Iweka et al. (2026) reports that the richness of the oil crop seeds is equal to the soil composition in a particular region. Furthermore, a fuel's standard and propensity to knock are determined by its cetane number. This helps indicate a fuel's combustion quality. The HHV of 40.36 MJ/kg is within a satisfactory range, and the cetane number of 59.76 is satisfactory for Jatropha seed biomass oil. As a result, OJSO's cetane number and HHV are both higher than the cetane number of 43.42 and the HHV of 39.4 MJ/kg from rubber seed biomass oil documented by Onoji et al. (2016). This indicates that the OJSO content is not only in line with neem seed bio-oil documented by Ugye et al. (2025), but it is also within the ASTM bound.

Table 9: Physical and Chemical Grades of OJSO

Properties	OJSO	(Haq et al., 2023) Pakistan	(Maftuchah et al., 2020) Indonesia	(Yusuff, 2021) Ado-Ekiti	(Emil et al., 2010) Thailand	(Emil et al., 2010) Malaysia	(Onoji et al., 2016) Iyanomo
Output (wt.%)	62.66	32.5	47.58	58.98	64.23	63.16	49.4
Moisture value (%)	0.002	-	-	-	-	-	1.73
Density (kg/m^3)	894	917	-	915.5	902.4	902.7	886.0
Viscosity	31.24	-	-	37.80	39.20	47.50	40.2
Specific gravity (g/cm^3)	0.890	0.916	-	0.9161	-	-	0.909
Acid content (mg KOH/g)	6.52	26.40	6.14+1.08	11.20	3.38	4.46	18.2
Free fatty content (mg KOH/g)	3.26	13.20	3.09+0.54	5.56	1.69	2.23	9.1
Peroxide (mg O_2/kg)	5.74	1.91	-	-	1.08	1.93	10.5
Iodine (g I_2/100g oil)	62.52	-	-	102.21	92.53	103.62	137.0
Saponification value (mg KOH/g)	198.31	213.5	217.39	188.83	216.09	193.55	195.30
Cetane number	59.76	-	-	-	-	-	43.42
HHV (MJ/kg)	40.36	-	-	-	-	-	39.4
Refractive index	1.432	-	-	-	-	-	1.471

CONCLUSION

i. Biomass oil from non-edible materials is an eco-friendly approach to generating low-cost bio-lubricants, and it can serve as a feedstock for biodiesel to power machines.

ii. The ground Ozoro Jatropha seeds were thermally dehydrated at 169 ^oC in an oven, as depicted by the Thermogravimetric analyzer.

iii. The ground Ozoro Jatropha seeds were extracted using a Soxhlet device with n-hexane. BBD was used to design, predict, and optimize the crude biomass oil output, while RStudio was used to predict and validate the BBD predicted yield. The best experimental result was displayed at 60 minutes, 50 g OJS weight, and 230 mL n-hexane, yielding a response of 62.66 wt.% as the highest centre-point and 47.30 wt.% as the mean optimum point. The BBD yields were validated with RStudio predictive tools. Thus, this study can be scaled up at an industrial level by utilizing 1:4 of OJS weight to solvent (n-hexane) volume at 60 minutes for a robust oil yield. Additionally, this work revealed that OJS weight and n-hexane, their coefficient and quadratic terms, were influential, unlike time. The R^2 of RStudio and the Box-Behnken-type Design are in alignment at 98.37%, even though RStudio processing capability yielded a p-value of $1.953e^{-05}$ which is lower than Box-Behnken-type Design `s p-value of <0.0001. Furthermore, RStudio`s visualization plots aligned with the derived BBD visualization plots, making the BBD an ideal experimental tool for optimizing and predicting crude biomass oil yield, while the RStudio tool is ideal for predicting crude biomass oil yield.

iv. The FTIR revealed the existence of triglyceride bio-oil, protein, and lignocellulosic carbohydrate, indicating a more unsaturated oil content in contrast to saturated oil content, as corroborated by the peroxide and Iodine contents. The seed`s HHV and LHV of 30.167 MJ/kg and 29.936 MJ/kg, respectively, revealed that the seed could serve as solid biomass fuel. Additionally, complementary TGA and FTIR characterization confirmed that the seed matrix is compositionally suited to solvent extraction, being dominated by an organic fraction (lipid, protein, and carbohydrate) that decomposes/dissolves preferentially, with only a small residual ash fraction remaining after the process.

v. Furthermore, the fuel grades of the biomass oil, such as HHV, cetane number, viscosity, and moisture values, suggest that it is combustible; hence, it has good potential as biodiesel feedstock for the betterment of both humans and the environment. Note that the utilization of this crude biomass oil will boost the local economy and promote a greener ecosystem, prompting unengaged citizens to become self-engaged or by crude biomass oil industries.

DECLARATION

Ethics Approval and Consent to Participate

This study was on conversion of non-edible biomaterials (waste) to biomass oil for lubrication and for biodiesel production to power machines and equipment. Additionally, the author have agreed to be held responsible for the contents of this manuscript and have approved the submission.

DATA AVAILABILITY

Datasets are available on request.

Author Contributions

Sunday Chukwuka Iweka: Conceptualization, Writing - original draft, Resources, Investigation, Writing - review & editing, Methodology, Validation, Formal analysis.

COMPETING INTERESTS

There are no conflicts of interest for the author.

FUNDING

This research did not receive funding.

REFERENCES

Abiodun, O., & Betiku, E. (2022). A novel heterogeneous catalyst synthesis from agrowastes mixture and application in transesterification of yellow oleander-rubber oil : Optimization by Taguchi approach. Fuel, 312(October 2021), 122999. https://doi.org/10.1016/j.fuel.2021.122999

Alhassan, M., Almustapha, M. N., Mohammed, M. L., Lawal, A. M., Adamu, M., & Shamsideen, U. (2024). PRODUCTION OF BIOLUBRICANT BLEND FROM JATROPHA CURCAS OIL. FUDMA JOURNAL OF SCIENCES, 7(6), 14–22. https://doi.org/10.33003/fjs-2023-0706-2168

Alpandi, A., Husin, H., Sidek, A., & Abdurrahman, M. (2022). Characterization of Malaysian Jatropha Seed Oil and Discovering the Process of Powdered Jatropha Leaves. Processes, 10(12), 2577. https://doi.org/10.3390/pr10122577

Ashine, F., Balakrishnan, S., Kiflie, Z., Bachheti, R. K., & Tizazu, B. Z. (2022). Parametric Optimization of Argemone Mexicana Seed Oil Extraction by Box-Behnken Experimental Design and the Oil Characteristics. https://doi.org/10.2139/ssrn.4157196

Ceran, Z. D., Demir, V., & Akgün, M. (2025). Optimization and kinetic study of biodiesel production from Jatropha curcas oil in supercritical methanol environment using ZnO/γ-Al2O3 catalyst. Biomass Conversion and Biorefinery, 15(3), 3903–3914. https://doi.org/10.1007/s13399-024-05307-9

Emil, A., Yaakob, Z., Satheesh Kumar, M. N., Jahim, J. M., & Salimon, J. (2010). Comparative Evaluation of Physicochemical Properties of Jatropha Seed Oil from Malaysia, Indonesia and Thailand. Journal of the American Oil Chemists' Society, 87(6), 689–695. https://doi.org/10.1007/s11746-009-1537-6

Ferreira, S. L. C., Bruns, R. E., Ferreira, H. S., Matos, G. D., David, J. M., Brandão, G. C., da Silva, E. G. P., Portugal, L. A., dos Reis, P. S., Souza, A. S., & dos Santos, W. N. L. (2007). Box-Behnken design: An alternative for the optimization of analytical methods. Analytica Chimica Acta, 597(2), 179–186. https://doi.org/10.1016/j.aca.2007.07.011

Fortunate, O., & Kishore, N. (2021). Computational Fluid Dynamics Investigation on Catalytic Hydrodeoxygenation of a Bio-Oil Model Compound in a Fluidized Bed Reactor. Journal of Thermal Science and Engineering Applications, 13(6). https://doi.org/10.1115/1.4050565

Haq, A., Laiq Ur Rehman, M., Rana, Q. ul A., Khan, A., Sajjad, W., Khan, H., Khan, S., Shah, A. A., Hasan, F., Ahmed, S., Islam, A., Badshah, M., Shah, T. A., Dawoud, T. M., & Bourhia, M. (2023). Production, optimization, and physicochemical characterization of biodiesel from seed oil of indigenously grown Jatropha curcas. Frontiers in Energy Research, 11. https://doi.org/10.3389/fenrg.2023.1225988

Hassan, M. (2022). A simulation of energy generation from Jatropha solid residues in a power plant in Jazan city, KSA. Heliyon, 8(5), e09352. https://doi.org/10.1016/j.heliyon.2022.e09352

Iweka, S. C., Akpomedaye, O., Emu, A. O., & Adepoju, T. F. (2024). Impact of optimization parameters on green sustainable oil from ripe palm kernel seeds for energy utilities: A machine learning approach. Scientific African, 23, e02097. https://doi.org/10.1016/j.sciaf.2024.e02097

Iweka, S. C., Chukwuneke, J. L., & Chinwuko, E. C. (2025a). Bio-lubricant production from Ozoro yellow oleander seeds and its industrial applications: Central composite design and python approach. Scientific African, 29, e02827. https://doi.org/10.1016/j.sciaf.2025.e02827

Iweka, S. C., Chukwuneke, J. L., & Chinwuko, E. C. (2025b). Thermodynamics and the Fuel Qualities of Produced Biodiesel From Nonedible Biomaterials: RStudio and Central Composite Design Approach. Energy Science & Engineering, 13(6), 3276–3295. https://doi.org/10.1002/ese3.70102

Iweka, S. C., Ozioko, F. C., Edafiadhe, E. D., & Adepoju, T. F. (2023). Bio-oil production from ripe pawpaw seeds and its optimal output: Box-Behnken Design and Machine Learning approach. Scientific African, 21, e01826. https://doi.org/10.1016/j.sciaf.2023.e01826

Iweka, S. C., Wodi, C., Okafor, E. E., Ewenkineyane, N. O., Ewunokan, G., & Iteme, K. O. (2026). Optimization, ignition point, and thermodynamic properties of rubber seed bio-oil: Python and <scp>RStudio</scp> approach. Environmental Progress & Sustainable Energy. https://doi.org/10.1002/ep.70512

Keneni, Y. G., Bahiru, L. A., & Marchetti, J. M. (2021). Effects of Different Extraction Solvents on Oil Extracted from Jatropha Seeds and the Potential of Seed Residues as a Heat Provider. BioEnergy Research, 14(4), 1207–1222. https://doi.org/10.1007/s12155-020-10217-5

Kethobile, E., Ketlogetswe, C., & Gandure, J. (2020). Torrefaction of non - oil Jatropha curcas L. (Jatropha) biomass for solid fuel. Heliyon, 6(12), e05657. https://doi.org/10.1016/j.heliyon.2020.e05657

Khater, E.-S. G., AbdAlla, S. A., Bahnasawy, A. H., & AbuHashish, H. M. (2024). Improvement of the production of bio-oil and biodiesel from Egyptian Jatropha seeds by using microwave and ultrasonic. Scientific Reports, 14(1), 1882. https://doi.org/10.1038/s41598-024-51579-6

Khemthong, C., Suttisansanee, U., Chaveanghong, S., Chupeerach, C., Thangsiri, S., Temviriyanukul, P., Sahasakul, Y., Santivarangkna, C., Chamchan, R., Aursalung, A., & On-nom, N. (2024). Physico-functional properties, structural, and nutritional characterizations of Hodgsonia heteroclita oilseed cakes. Scientific Reports, 14(1), 19241. https://doi.org/10.1038/s41598-024-70276-y

Maftuchah, Zainudin, A., Winaya, A., & Rahmadesi, Y. (2020). Biodiesel generated from Jatropha (Jatropha curcas Linn.) seeds selected based on various genotypes crossbred. Energy Reports, 6, 345–350. https://doi.org/10.1016/j.egyr.2020.11.160

Nandiyanto, A. B. D., Oktiani, R., & Ragadhita, R. (2019). How to Read and Interpret FTIR Spectroscope of Organic Material. Indonesian Journal of Science and Technology, 4(1), 97. https://doi.org/10.17509/ijost.v4i1.15806

Nyorere, O., Oluka, S. I., Onoji, S. E., Nwadiolu, R., & Adepoju, T. F. (2024). Production of biodiesel from biocatalysis of agro-wastes in acidic environment. Scientific African, 24, e02154. https://doi.org/10.1016/j.sciaf.2024.e02154

Odetoye, T. E., Afolabi, T. J., Abu Bakar, M. S., & Titiloye, J. O. (2018). Thermochemical characterization of Nigerian Jatropha curcas fruit and seed residues for biofuel production. Energy, Ecology and Environment, 3(6), 330–337. https://doi.org/10.1007/s40974-018-0104-0

Oehlschlaeger, M. A., Wang, H., & Sexton, M. N. (2013). Prospects for Biofuels: A Review. Journal of Thermal Science and Engineering Applications, 5(2). https://doi.org/10.1115/1.4023602

Onoji, S. E., Iyuke, S. E., & Igbafe, A. I. (2016). Hevea brasiliensis (Rubber Seed) Oil: Extraction, Characterization, and Kinetics of Thermo-oxidative Degradation Using Classical Chemical Methods. Energy & Fuels, 30(12), 10555–10567.

https://doi.org/10.1021/acs.energyfuels.6b02267

R.S. Ugye, I. Garba, & S.U. Muhammad. (2025). Evaluation of Physicochemical Properties of Bio-Lubricant Locally Produced from Nigerian Neem Oil (Engine Oil Application). Journal of Innovations in Engineering and Technology Research. https://doi.org/10.70382/hujcer.v8i5.007

Riayatsyah, T. M. I., Sebayang, A. H., Silitonga, A. S., Padli, Y., Fattah, I. M. R., Kusumo, F., Ong, H. C., & Mahlia, T. M. I. (2022). Current Progress of Jatropha Curcas Commoditisation as Biodiesel Feedstock: A Comprehensive Review. Frontiers in Energy Research, 9. https://doi.org/10.3389/fenrg.2021.815416

Ruatpuia, J. V. L., Halder, G., Vanlalchhandama, M., Lalsangpuii, F., Boddula, R., Al-Qahtani, N., Niju, S., Mathimani, T., & Rokhum, S. L. (2024). Jatropha curcas oil a potential feedstock for biodiesel production: A critical review. Fuel, 370, 131829. https://doi.org/10.1016/j.fuel.2024.131829

Silva, J. J. F., Vieira Júnior, C. M., Bôa-Viagem, H. L., Silva, V. dos S., Santos, H. da S., & Silva, S. P. R. (2020). Chemical and energetic characterization of Jatropha Curcas seed after two years in stock. Brazilian Journal of Development, 6(6), 33229–33237. https://doi.org/10.34117/bjdv6n6-033

Suttibak, S., Saengmanee, C., & Chuntanapum, A. (2024). Production of bio-oil from Tung seed residues in a fluidized-bed reactor. Heliyon, 10(7), e28310. https://doi.org/10.1016/j.heliyon.2024.e28310

Yusuff, A. S. (2021). Parametric optimization of solvent extraction of Jatropha curcas seed oil using design of experiment and its quality characterization. South African Journal of Chemical Engineering, 35, 60–68. https://doi.org/10.1016/j.sajce.2020.11.006